Advanced Methods and Materials for Vat Photopolymerization Additive Manufacturing

Carl J. Thrasher

A thesis

submitted in partial fulfillment of the

requirements for the degree of

Master of Science

University of Washington

2017

Committee:

Andrew J. Boydston

Alshakim Nelson

Program Authorized to Offer Degree:
Chemistry

©Copyright 2017

Carl J. Thrasher

University of Washington

Abstract

Advanced Methods and Materials for Vat Photopolymerization Additive Manufacturing

Carl J. Thrasher

Chair of the Supervisory Committee:
Dr. Andrew J. Boydston
Chemistry

Vat photopolymerization is a versatile 3D printing technology for rapid prototyping applications. Recent innovations have made vat photopolymerization technologies vastly cheaper and more accessible, but the field still faces numerous shortcomings. Notably, the lack of materials and multi-material printing make vat photopolymerization unsuitable for many advanced rapid prototyping applications. Advancements in methodology and materials which attempt to address these shortcomings are discussed herein. More specifically, printing hydrophobic resins, gradient material compositions, multi-material objects, and materials with high elongation are explored. This research is anticipated to help bring the capabilities of vat photopolymerization to new application fields such as soft robotics, wearable devices, and flexible electronics.

TABLE OF CONTENTS

LIST OF FIGURES

Figure Number Page

LIST OF TABLES

Table Number Page

ACKNOWLEDGEMENTS

I wish to express my sincerest thanks to all of the members of the Boydston Group present during my time at the University of Washington. In addition to being incredible and inspiring chemists, you have become like family. I very much cherish my time here and could not have imagined a more rewarding experience. I hope to work with you in the future and that I will see you again soon. I would also like to express my thanks to Dr. Ahbijit Saha of the Nelson Group and Bill Kuykendall from the Mechanical Engineering Department for help in data collection.

DISCLAIMER

The views expressed in this article are those of the author and do not reflect the official policy or position of the United States Air Force, Department of Defense, or the U.S. Government.

Chapter 1. Introduction

The rapid expansion of additive manufacturing is challenging the notions of when, where, what and how devices can be fabricated on demand.[1-15] Additive manufacturing, commonly referred to as 3D printing, has found use in fields such as the aerospace industry, medicine, dentistry, consumer electronics, and many more.[16,17] This widespread success is in large part due to cheap and user-friendly technology, but it also due to the fact that additive manufacturing can ostensibly operate without regard to the complexity of 3D geometries being fabricated.[18] To date, one of the most industrially relevant forms of additive manufacturing is vat photopolymerization, often termed stereolithography.[19] Vat photopolymerization involves the use of directed irradiation to polymerize a vat of photoactive resin, curing a 3D object in a layer-by-layer fashion. The ability to control light is the primary determinant of both the speed and resolution of vat photopolymerization. With sufficiently advanced optics systems that are commercially available, vat photopolymerization excels in these categories compared to other methods of 3D printing.[20] Unfortunately, vat photopolymerization is performance inhibited in other areas which significantly detract from its usefulness.

In particular, vat photopolymerization is material starved and has limited access to multi-material printing capabilities. The vast majority of 3D printing photoresins available are hard, brittle plastics with little flexibility.[6] Some high performance materials have been reported, but

they use proprietary resins and require special printing technology.[21] Some flexible resins have been reported, but with elongations to break only up to 100% strain they have limited application.[22-23] Additionally, printing with multiple materials is a difficult endeavor for vat photopolymerization technologies, as the vat must be switched mid-print. Automatic vat switching technologies have been demonstrated, but they introduce large tradeoffs in speed and cost for limited functionality.[24] The need to clean between each layer of new material limits the practicality of multi-material vat photopolymerization, as does the inability to control the material composition in the xy plane of a layer. Strategies for improving vat photopolymerization, especially in regard to material deficits and multi-material printing, are discussed herein.

The second chapter reviews state of the art methodologies for vat photopolymerization and then expounds upon new innovations to the field. Experiments demonstrating proof of concept and evaluating performance are discussed. One methodology explored is that of single-vat multi-material photopolymerization using selective energy inputs. Two forms of this idea are evaluated; one exploits photochemistries with different kinetic behavior to provide spatial control over material composition while the other relies on orthogonal photochemistries with selective activation by different wavelengths of light. Both forms of multi-material printing could yield multi-material vat photopolymerization capable of producing parts with full spatial control of material composition as well as truly gradient material property sets. Another methodology illustrated herein is the concept of printing at the biphasic interface of two immiscible liquids. This concept is hypothesized to hold numerous benefits in regards to printability and to provide access to photoresins which are otherwise incompatible with vat photopolymerization.

The third chapter focuses on elastomer photoresins for vat photopolymerization. It details the chemical principles holding back most elastomer photopolymerizations from printability and suggests a new paradigm of producing elastomeric structures by vat photopolymerization. Various resins and printing conditions are explored, culminating in a modular set of chemistries to access printable photoresins with predetermined property sets. The viability, relevance, and performance of these resins are explored through the creation of a multi-material soft-robotic actuator.

Notes to Chapter 1

1. Gross, B. C., Erkal, J. L., Lockwood, S. Y., Chen, C. & Spence, D. M. Evaluation of 3D Printing and Its Potential Impact on Biotechnology and the Chemical Sciences. *Anal. Chem.* **86,** 3240–3253 (2014).
2. Gross, B., Lockwood, S. Y. & Spence, D. M. Recent Advances in Analytical Chemistry by 3D Printing. *Anal. Chem.* **89,** 57–70 (2016).
3. Melchels, F. P. W., Feijen, J. & Grijpma, D. W. A review on stereolithography and its applications in biomedical engineering. *Biomaterials* **31,** 6121–6130 (2010).
4. Melchels, F. P. W. *et al.* Additive manufacturing of tissues and organs. *Prog. Polym. Sci.* **37,** 1079–1104 (2012).
5. Stansbury, J. W. & Idacavage, M. J. 3D printing with polymers: Challenges among expanding options and opportunities. *Dent. Mater.* **32,** 54–64 (2016).
6. Leu, M. C. & Arbor, A. Additive Manufacturing: Current State, Future Potential, Gaps and Needs, and Recommendations. *J. Manuf. Sci. Eng.* **137,** 1–10 (2016).
7. Tumbleston, J. R. *et al.* Continuous liquid interface production of 3D objects. *Science* **347,** 635–639 (2008).
8. Sun, C., Fang, N., Wu, D. M. & Zhang, X. Projection micro-stereolithography using digital micro-mirror dynamic mask. *Sensors Actuators A* **121,** 113–120 (2005).
9. Zheng, X. *et al.* Design and optimization of a light-emitting diode projection micro-stereolithography three-dimensional manufacturing system. *Rev. Sci. Instrum.* **83,** (2015).
10. Patel, D. K., Sakhaei, A. H., Layani, M., Ge, Q. & Magdassi, S. Highly Stretchable and UV Curable Elastomers for Digital Light Processing Based 3D Printing. *Adv. Mater.* (2017). doi:10.1002/adma.201606000
11. Zarek, M. *et al.* 3D Printing of Shape Memory Polymers for Flexible Electronic Devices. *Adv. Mater.* **28,** 4449–4454 (2016).
12. Ge, Q. *et al.* Multimaterial 4D Printing with Tailorable Shape Memory Polymers. *Sci. Rep.* **6,** 31110 (2016).
13. Wu, W., Deconinck, A. & Lewis, J. A. Omnidirectional Printing of 3D Microvascular Networks. *Adv. Healthc. Mater.* 178–183 (2011). doi:10.1002/adma.201004625
14. Truby, R. L. & Lewis, J. A. Printing soft matter in three dimensions. *Nature* **540,** 371–378 (2016).
15. Mannoor, M. S. *et al.* 3D printed bionic ears. *Nano Lett.* **13,** 2634–2639 (2013).

16. Gilpin, Lyndsey. 10 industries 3D printing will disrupt or decimate. TechRepublic. (2014). Available at http://www.techrepublic.com/article/10-industries-3d-printing-will-disrupt-or-decimate/ (Accessed March 2017).

17. Stratasys. Industries. Stratasys Ltd. Available at http://www.stratasys.com/industries (Accessed March 2017).

18. Zheng, X. *et al.* Ultralight, Ultrastiff Mechanical Metamaterials. *Science* **344,** 1373–1377 (2014).

19. Grunewald, Scott. Global 3D Printer Market Up 19% in 2015 as Industrial and Commercial 3D Printer Sales Drop, XYZprinting Remains on Top. 3Dprint.com. (2016). Available at https://3dprint.com/128648/global-3d-printer-market-up/ (Accessed March 2017)

20. Aniwaa. Fast 3D printing. Aniwaa Pte. Ltd. (2016). Available at http://www.aniwaa.com/fast-3d-printing/ (Accessed March 2017)

21. Carbon3D. Carbon3D Materials. Available at: http://www.carbon3d.com/materials. (Accessed March 2017)

22. Spot A Materials. Spot-E Elastic. Available at: http://spotamaterials.com/product/spot-e-1kg/ (Accessed March 2017)

23. Formlabs. Formlabs Flexible. (2017). Available at: https://formlabs.com/materials/engineering/#flexible (Accessed March 2017)

24. Zhou, C., Chen, Y., Yang, Z., & Khoshnevis, B. Development of a Multi-material Mask-Image-Projection-based Stereolithography for the Fabrication of Digital Materials. *Proc Solid Freeform Fabr.* Austin, TX, 65-80 (2011).

Chapter 2. Methods of Vat Photopolymerization

2.1. Introduction

Vat photopolymerization involves the use of directed irradiation to polymerize a vat of photoactive resin, curing a 3D object in a layer-by-layer fashion. This can be accomplished in many ways, and as such the ASTM supported term vat photopolymerization can encompass various additive manufacturing technologies.[1] The first mature vat photopolymerization system was coined stereolithography by Chuck Hull in 1986 who proceeded to found 3D Systems based on this technology.[2] His original process used a UV laser which was oriented over and drawn across a vat in a pre-programmed pattern, photocuring any photopolymer that it illuminated. In this vat a build stage is used as a lower boundary for the first layer, and it is moved slightly lower (the height of a single layer) after each layer is complete to cover the cured polymer with new photoresin (Figure 2.1). After numerous iterations, an object will have been fabricated in a layer-by-layer fashion. Modern stereolithography (SLA) systems work much like the original design, although instead of a top-down approach they can also operate in a bottom-up approach. The only difference is that in a bottom-up approach the light will travel up through a transparent container to the build stage, which now acts as an upper-boundary and moves up for each new layer (Figure 2.2).

Another variation of vat photopolymerization uses digital light processing (DLP) technology to illuminate the photopolymer. In typical DLP systems, 3D models are sectioned into thin slices, or layers, which are represented by a series of black and white images. Objects are printed by sequential projection of each image into a vat of photoresin as the build stage moves away after each layer. In terms of speed, the ability to polymerize an entire layer at once is a significant improvement to the aforementioned laser systems which must raster the pattern of each layer. One might expect a concurrent loss in resolution with such an increase in speed, but the manipulation of light with DLP technology can be just as precise as laser based technology.[3] Because DLP equipment is widely available commercially in the form of projectors, DLP additive manufacturing (DLP-AM) is making vat photopolymerization vastly more accessible. The prevalence of vat photopolymerization has been steadily increasing, especially for consumer grade systems, as seen in Table 2.1.[4] The most advanced form of vat photopolymerization to date has been termed continuous liquid interface production or CLIP printing.[5] Pioneered by Joseph DeSimone and the basis of the company Carbon3D Inc,[6] this style of vat photopolymerization can operate significantly faster than other vat photopolymerization methods. This is because this style of vat photopolymerization prints continuously instead of sequentially producing discrete layers. The innovation which enables CLIP printing is the use of a gas permeable bottom layer in a bottom-up vat photopolymerization setup. The permeable bottom layer will diffuse oxygen, a radical inhibitor, to a concentration such that photopolymerization does not occur directly adjacent to the bottom layer, but rather some height above the bottom layer where the concentration of oxygen is less. This allows for the interface where solidification of resin occurs to always be between liquids rather than between a liquid and a solid. The liquid interface

ensures that resin is always available to print as an object is pulled up, while other similar systems must wait for resin to refill underneath the object to resume printing.

Vat photopolymerization of objects with homogenous materials has been facilely demonstrated in numerous variations, however, processes to fabricate objects with heterogeneous materials through vat photopolymerization are quite underdeveloped in comparison to other 3D printing methods. The first and only method of multi-material vat photopolymerization relies on changing the vat for each new instance of material. Even in systems where the vat exchange is automated, this method of fabrication is slowed dramatically by the switching and cleaning process.[7] In addition, this method is incapable of producing material gradients as the materials must appear in quantized amounts according to the resolution of the printer. Furthermore, vat exchange can only reliably control the spatial variation of materials along the z-axis if using a bottom-up approach. This is because exchanging a vat to a new material after only part of a layer is polymerized can cause air bubbles to become entrapped and no material will be cured as light is illuminated onto the space where the air is occupying. A top-down approach can resolve this issue, but this drastically increases the resin needed to print and makes the cleaning between each exchange much more difficult. Boydston et al. recently demonstrated that by controlling the intensity of light used to polymerize each layer, the cross-link density of the resulting polymer could be altered.[8] This method of achieving heterogeneous materials does not suffer from limited spatial control or inability to create gradients and is able to vary mechanical properties, such as the storage modulus, of printed objects by over 30%. For applications requiring larger differences or ranges of other properties however, this method is unsuitable. As evidenced by the success of many other forms of multi-material printing, multi-material vat photopolymerization

would be a desirable and advantageous capability.[9] To make multi-material vat photopolymerization successful, significant leaps in capabilities will be required.

To improve upon current vat photopolymerization processes, new innovations are needed. We present two paradigms to achieve multi-material vat photopolymerization capable of fast printing, full spatial control of material composition, and the ability to produce gradients. Furthermore, we explain and demonstrate a method of enhancing the printing of hydrophobic resins, elaborating on the benefits and opportunities which this method can give rise to.

2.2. Multi-material Vat Photopolymerization

Multi-material and graded printing capabilities are highly desirable and have been demonstrated in various forms. And although these capabilities exist, integrating them into a vat photopolymerization process could yield several advantages. For example, material extrusion of preformed thermoplastic filaments has been adapted to allow for mixing of different filaments during the extrusion process.[10] This method is marred by many limitations. While multiple nozzles may be used to deposit different materials, truly graded parts are impossible to achieve as the thermoplastic materials exhibit macroscopic separation. This separation also leads to delamination at material interfaces and severely inhibits final product quality. Further, the scope of available materials, both commercial and custom, is also quite small. Both binder jetting and photopolymer jetting 3D printing technologies have significant multi-material capabilities, but are extremely expensive (ranging from $50,000-2 million) and operate through proprietary (i.e., "closed") systems.[11,12] They also face significant engineering restraints in the form of resin viscosity and complex equipment that requires professional care and maintenance.[13,14] Vat photopolymerization, on the other hand, is relatively inexpensive, mechanically simple, and can be operated with free, open-source software. If accomplished in a single vat instead of using

cumbersome vat exchange technology, multi-material vat photopolymerization would be an excellent tool to quickly and cheaply produce objects with full spatial control of material composition as well as the potential for true material gradients.

To incorporate multiple material types during vat photopolymerization, non-interacting, or orthogonal, polymerizations must be used in the same resin mixture. When using multiple orthogonal polymerizations, the resulting material is comprised of intertwined, but chemically separate networks. A common example of this type of polymerization taken to completion is the formation of dual-network epoxy-acrylate systems. In a mixture of epoxy and acrylate monomers, epoxy monomers can be polymerized using a slow cationic mechanism while acrylates can be polymerized using a fast radical mechanism.[15] By adapting these polymerizations to photopolymerizations and using suitable materials, it would be possible to dictate the material composition by varying the amount of irradiation, or light intensity, to take advantage of differences in kinetic reactivity as shown in Figure 2.3. If light stimulates the resin for only a short amount of time, the printed area will be comprised primarily of the monomer of the highest polymerization rate ("polymerization rate" is used here as a general embodiment of all relevant processes: photoactivation, initiation, and propagation). If the resin is exposed for a long time, however, both monomers will polymerize and a dual-network material results. Applying this to a layer-by-layer method would then yield a form of multi-material additive manufacturing through DLP technology.

Under this type of multi-material vat photopolymerization system, the four main factors that need to be kept in mind are the layer curing times, the light intensity, the monomer feed ratios, and the difference in material properties of the two monomer systems. As acrylates are known for their extremely fast photopolymerizations, they are suitable to

serve as the kinetically fast monomer in a mixed vat of resin. The range of available properties would then be dictated by the differences in properties between the acrylic base polymer network and the dual-network system. Cationic epoxy photopolymerizations are strong candidates for the second monomer in a dual-network as they have been well-studied, and generally have slower polymerization kinetics than acrylate systems.[16,17] Many mechanisms exist to alter the kinetic profiles of polymerization of epoxy systems such as changing monomer type, photoinitiator type, and using multipart photoinitiator systems. These methods can be used to make the epoxy polymerization kinetically suitable for DLP-AM, as too long of curing times could lead to ill-defined objects and prohibitively long printing sessions. In this form of multi-material printing, objects with hard-to-soft material changes function as excellent proof of concept demonstrations. As epoxy polymers tend to be hard and brittle, soft, tough, and flexible acrylate monomers can be paired to enhance contrast.[15] By varying the time of cure along a gradient for each layer, objects with property gradation ranging from soft (short cure times) to hard (long cure times) can be fabricated.

One possible chemical combination which is compatible with this type of printing is to use a mixture of 3,4-epoxycyclohexylmethyl 3,4-epoxycyclohexanecarboxylate (a cationically initiated monomer) and 2-hydroxyethyl acrylate (a radical initiated monomer) with triarylsulfonium hexafluoroantiminate and Irgacure 819 as cationic and radical photoinitiators respectively. Unlike many radical cation forming photoinitiators, triarylsulfonium hexafluoroantiminate will not interact with most other photoactive species such as Irgacure 819 (although they will interact will acrylic monomers), which helps enhance orthogonality.[18] Preliminary experiments show that this mixture can be exposed to UV light of different amounts and that a large difference in hardness is achieved comparing

low exposure times (only radical polymerization) and long exposure times (both radical and cationic polymerization). To retain soft regions and avoid dark curing, it is prudent to terminate active chain ends and swell out potential monomer by soaking the object in a nucleophilic solvent such as methanol. It is also important to note that while differences in properties can be obtained, full separation of the two materials will never be achieved. An initial proof of concept photopolymerization was carried out with this combination of materials and it was noted that hard and soft regions could be reliably dictated by controlling exposure times.

Another, more advanced method of achieving multi-material vat photopolymerization is to use different wavelengths of light to polymerize different materials selectively in the same vat of resin (Figure 2.4). In this method, the projected photo-pattern will not only determine the exact spatial geometry of a print, but also a more complete control over the chemistry being used to dictate material composition (from 100% of resin-A, to a mix resin-A/resin-B, to 100% of resin-B). For this to be accomplished, both the initiation and the polymerization chemistry of the materials must be orthogonal. A potential system for multi-material printing could involve a similar mixed vat of radical and cationic (acrylate and epoxy) monomers to the previous example, but with different photoinitiators that only interact with one type of polymerization. If these photoinitiators activated at selective wavelengths, a projector could simply shine a specific color to determine whether epoxides, acrylates, or a gradient of both should be activated at that position. Successful implementation of this system in a layer-by-layer fashion would offer completely controlled multi-material DLP-AM.

The main challenge that must be studied and overcome in this system is identifying two orthogonal photoinitiators for the initiation step of polymerization. Many cationic

photoinitiators will interact with acrylate monomers as they form an initial radical in the form of a radical-cation prior to acid, or cation, generation.[19,20] Additionally, the absorbance spectra of most photoinitiators overlap in the UV or visible light spectrum, which means that those photoinitiators cannot be activated selectively. To pursue this type of fully orthogonal multi-material system, new photoinitiators must be identified. Recently reported ferrocenium-based systems have demonstrated cationic initiation when excited by light through a change in their ligand coordination or hapticity (Figure 2.5).[21,22] This change does not involve nor promote the formation of radical species. To be broadly usable, these photoinitiators must be modified to increase both their absorption and solubility. The absorbance range can be redshifted by extending the conjugation of the salts ligands while the solubility can be adjusted through the incorporation of solvent, monomers, surfactants, or by altering ligand polarity.

An example system to successfully execute this type of printing might use blue or near-UV light to activate a cationic ferrocenium salt while using red light to excite the free-radical photoinitiator H-Nu 640, which does not activate in blue light. The cationic system will only interact with a hard material-forming epoxide monomer, such as 3,4-epoxycyclohexylmethyl 3,4-epoxycyclohexanecarboxylate, while the H-Nu 640 would polymerize a rubber forming polyurethane diacrylate monomer, such as Ebecryl 8413. Printing could be conducted with a DLP projector, programming different colors to appear at different locations in space to achieve the desired multi-material print.

Because commercially-available and open-source printing software only allows for binary black and white photo-patterns and projections lasting for a uniform amount of time, options to control color or light intensity on a layer-to-layer basis must be evaluated. In order to

vary the cure time, light intensity, and ultimately wavelength (especially within single 2D layers), a program capable of controlling these variables is necessary. This would involve the use of custom image stacks and command series in place of a traditional printing operators. While this is technologically trivial, proper engineering and elegant g-code can greatly enhance printing quality and for that reason software development should not be approached carelessly.

2.3. Biphasic Vat Photopolymerization

First established by Carbon3D Inc,[23] biphasic vat photopolymerization consists of using a liquid that is immiscible with a photoresin as the bottom layer of your vat container as shown in Figure 2.6. In this way, a liquid monomer resin is rested on an immiscible, but wettable liquid of higher density in an optically transparent container such that a liquid-liquid interface is formed and separation is maintained. The printing can then proceed in either a top-down or bottom-up fashion as a normal vat photopolymerization process. There are several advantages to this printing setup, but one of the primary benefits is that it allows for easy printing of hydrophobic resins. Many hydrophobic resins, such as acrylated silicones, are unable to be printed normally because of the similarity to the non-stick silicone lining traditionally used for printing. When resin swells into the bottom lining, it will polymerize into the lining and pull off from the build stage. Removing the PDMS lining and using the glass vat as an interface is similarly not suitable as adhesion between printed parts and vat will pull the part off the build stage. Hydrophobic resins can be successfully printed using a top-down method or expensive fluorinated glassware, but these options are not consistently accessible. With biphasic vat photopolymerization, hydrophobic resins can be printed simply by adding water.

Many other advantages can come from using a biphasic system, in which a dense, inactive liquid is used as the bottom layer to separate the photoresin from the vat bottom. For

example, the bottom layer in a biphasic vat photopolymerization setup can act as a heat sink. By using a liquid with a higher thermal conductivity than the resin, heat from the exothermic photopolymerization can be directed downward through the inactive bottom layer instead of radially through the photoresin. This increases the surface area which is available to dissipate heat away from the photopolymerization. This will help insure consistent photopolymerization kinetics and hence printing accuracy/resolution. It can also allow for more exothermic reactions to take place, for more concentrated energy deposition to occur (which allows for faster kinetics, decreased layer times, and increased print speed), and for large surface area print layers to be printed without being affected by bulk heating effects.

Another possibility for biphasic vat photopolymerization is to control polymerization at the interface of the two liquids. Ways to enable this control include separating monomer from photoinitiator or separating photoinitiator from a photosensitizer/co-initiator by placing each part in the different liquids of the biphasic system. If photosystems are separated than polymerization will not occur except at the interface of the two liquids. This could be used to control the layer height of a print by monitoring the diffusion of an active radical species, potentially enabling extremely thin layers. It could also be leveraged to use initiators that have poor solubility in the resin mixture.

The intended use as described by Carbon3D's patent is to enable continuous printing conditions, similar to their CLIP printing technology.[23] Using a biphasic vat system is just another way of making sure polymerization occurs at a liquid interface. Biphasic vat photopolymerization has all the same benefits as CLIP printing, including fast resin infill and no potential for adhesion to the bottom of the build vat. It also benefits from being simpler than

CLIP printing in that it does not have to worry about the concentration of oxygen permeating through the bottom of the vat.

Another possible use of a biphasic system is to enhance top-down vat photopolymerization. One of the largest detractors from top-down vat photopolymerization systems is that they require a vast amount of resin, the depth of which must be greater than the object being printed. A biphasic mixture could be used in a top-down vat photopolymerization approach to reduce the amount of resin required per print. The top layer of liquid would be photoresin and the bottom layer would be a liquid of higher density. Light would be projected downward into the container of the biphasic mixture onto a build stage which is positioned such that it is just under the top layer of photoresin. As light is projected and a photopolymerized layer is solidified onto the build stage, the stage can be lowered further into the biphasic mixture such that only the top of the recently solidified layer is positioned in the layer of photoresin. In a biphasic mixture, the bulk of the container volume can be occupied by the higher density liquid and is ideally reusable or cheap. For example, if a hydrophobic resin is being printed, water can simply fill up most of the vat. This approach is also compatible with resin depth control processes. In an ideal depth control setup, the depth of the top layer resin would be exactly equal to the layer height. Minimizing resin depth in a controlled manner can eliminate light penetration constrictions and would allow for photopolymerization to occur on overhangs without curing deeper than intended. It is also useful for vat photopolymerization setups using high light intensities to increase print speeds.

To evaluate the feasibility of printing with a biphasic vat photopolymerization system, hydrophobic resin was printed on a layer of brine. The build vat consisted of a 400 mL Pyrex beaker with the top removed (inner diameter = 73 mm, height = 87 mm). The bottom sidewall of

this beaker was lined with a thin layer of poly(hydroxyethylacrylate) so as to eliminate contact between the resin and glass as it was found that the attraction between the two could push and partition away the bottom layer of liquid. This beaker was filled with 30 mL of brine and the build stage was leveled to the top surface of this liquid layer. Hydrophobic silicone resin was then placed on top of the brine such that it covered the entire surface. The printing process then continued as normal in a bottom-up fashion. Printing was found to be facile, highly repeatable, and produce accurate structures.

2.4. Conclusion

We have explored new innovative processes to improve the utility of vat photopolymerization. We presented two paradigms which can be implemented in vat photopolymerization systems to produce objects with full spatial control of material composition as well as truly gradient material property sets. Additionally, a method of printing using a biphasic system of immiscible liquids was explored. We expounded upon the numerous advantages of such a system, including the ability to print hydrophobic resins, continuous printing, passive temperature control, control of photoinitiation location, and the ability to reduce the amount of resin required to print in a top-down vat photopolymerization system. We expect these improvements will greatly increase the utility and capabilities of vat photopolymerization systems when they are fully integrated into a 3D printing system.

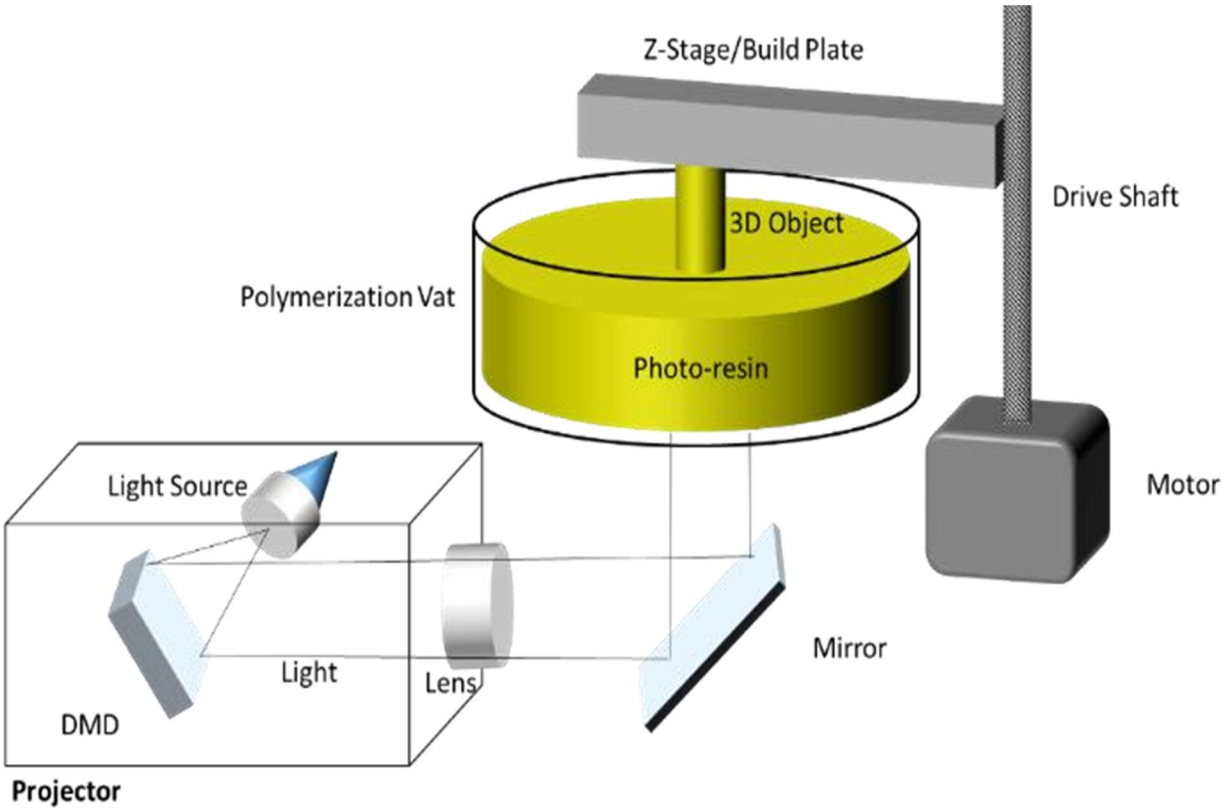

Figure 2.1. Schematic of a Vat Photopolymerization Setup. Process shown uses DLP technology in a bottom-up fashion. Objects are printed by sequential projection of images into the resin while raising the z-stage between each image.

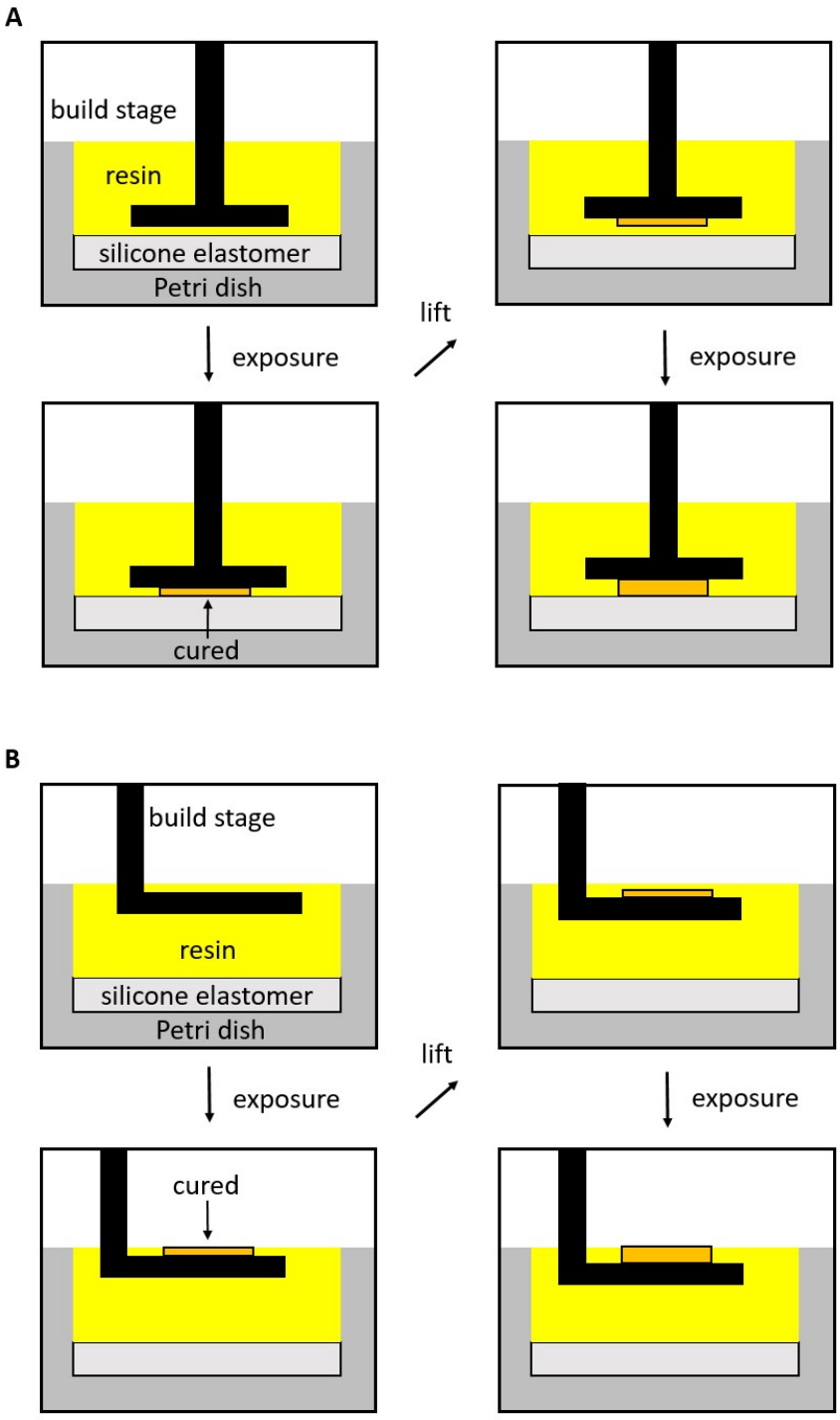

Figure 2.2. Bottom-up vs. Top-down Vat Photopolymerization. Workflow diagrams of A) bottom-up vat photopolymerization and B) top-down vat photopolymerization.

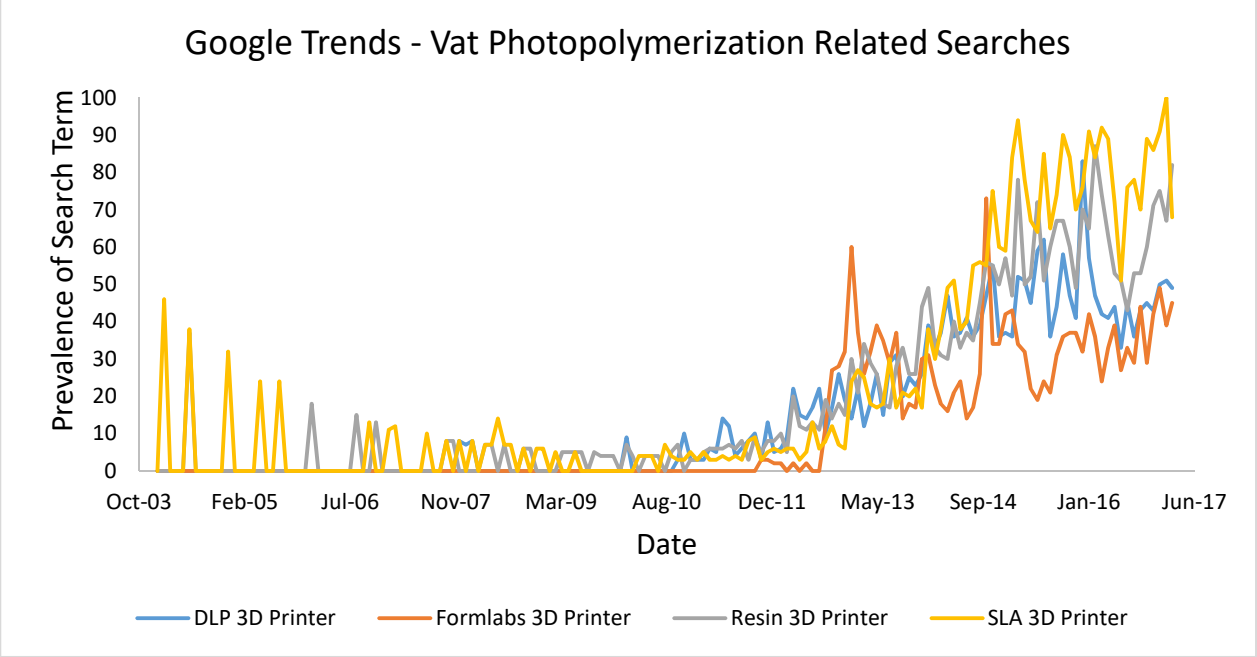

Figure 2.3. Growth of Vat Photopolymerization Data comparing the prevalence of search terms over time as accessed by Google Trends (March 2017).

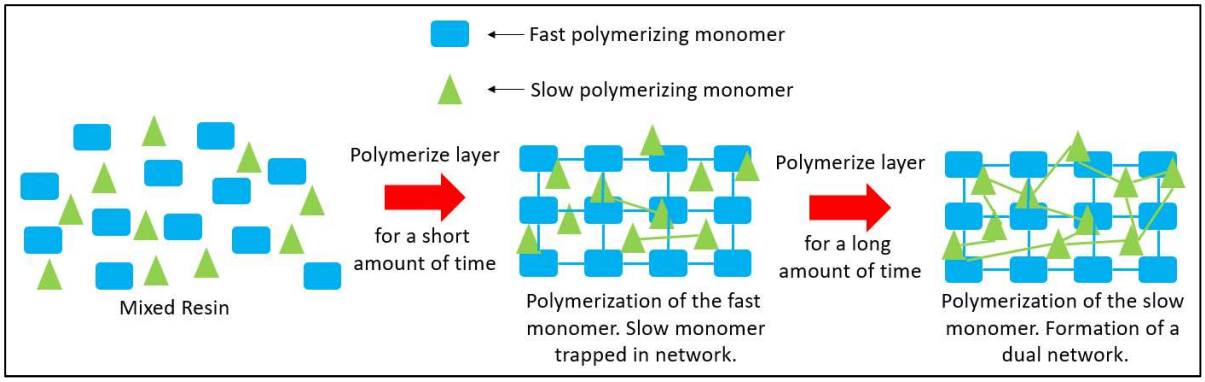

Figure 2.4. Sequential Photopolymerization of Slow and Fast Monomer Mixture. The process of multi-material photopolymerization controlled by exploiting the differential rates of polymerization of two photoactive systems is shown.

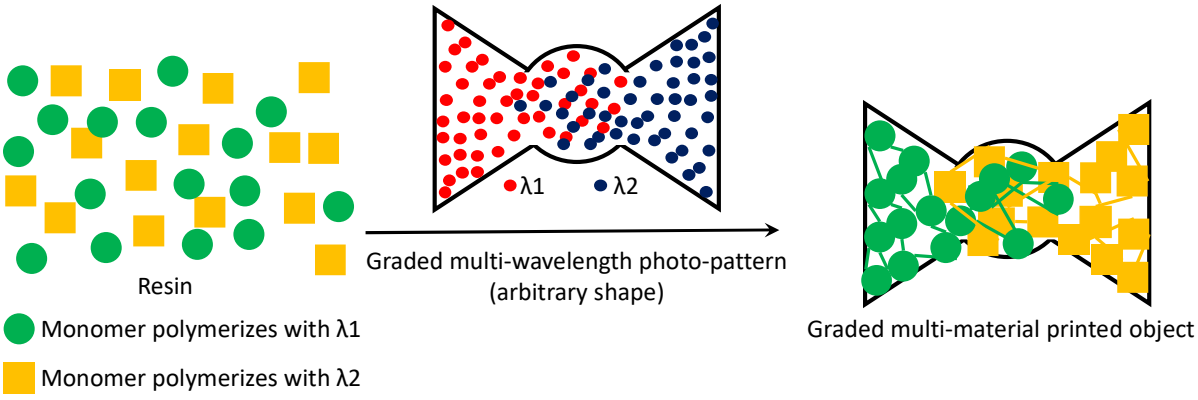

Figure 2.5. Simultaneous Photopolymerization of Selective Monomers. The process of multi-material photopolymerization of orthogonal photosystems by selective activation from different wavelengths of light.

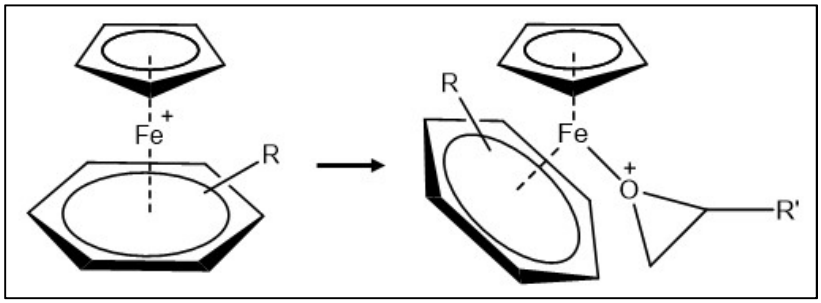

Figure 2.6. Hapticity Shift of Ferrocenium Salt. Schematic of typical hapticity shift of ferrocenium salt after exposure to light and accompanying ligation of an epoxide monomer.

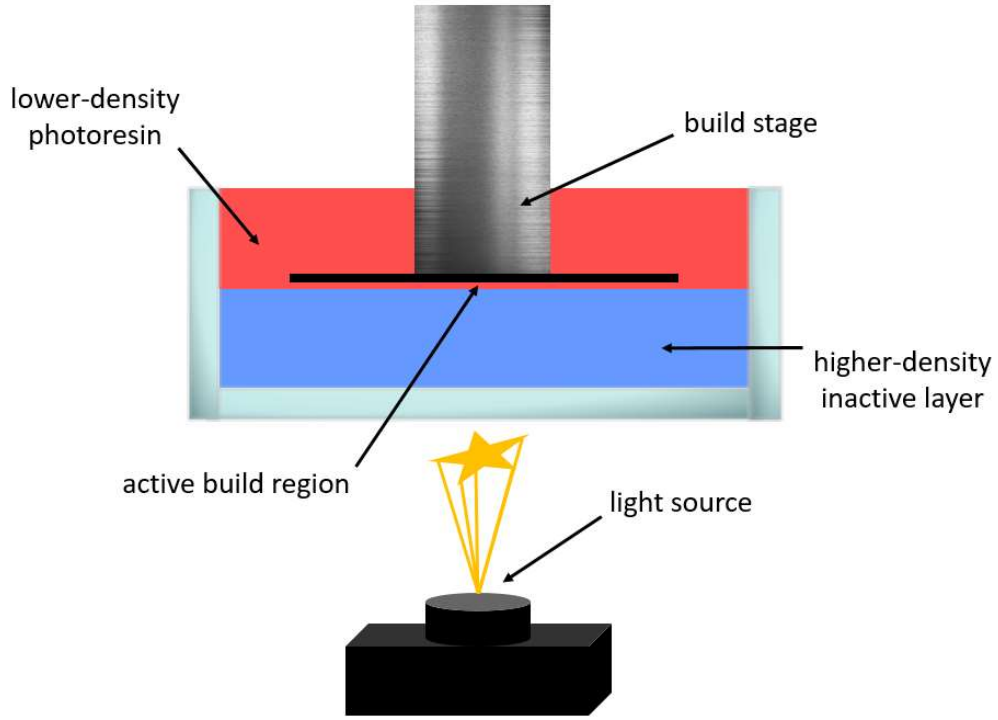

Figure 2.7. Biphasic Vat Photopolymerization Setup. Schematic of biphasic vat photopolymerization setup utilizing a bottom-up approach.

Notes to Chapter 2

1) ASTM 52910: Standard Guidelines for Design for Additive manufacturing. *American Society for Testing and Materials.* (2017).

2) Gibson, Ian, & Jorge Bártolo, Paulo. History of Stereolithography. *Stereolithography: Materials, Processes, and Applications.* 41-43 (2011).

3) Gauvin, R. *et al.* Microfabrication of complex porous tissue engineering scaffolds using 3D projection stereolithography. *Biomaterials.* **33**, 15, 3824-3834 (2012).

4) Kloski, Liza, & Kloski, Nick. *Make: Getting Started with 3D Printing.* (Maker Media, 1st ed, 2016).

5) Tumbleston, J. R. *et al.* Continuous liquid interface production of 3D objects. *Science* **347,** 635–639 (2008).

6) Carbon3D. Carbon3D Materials. Available at: http://www.carbon3d.com/materials (Accessed March 2017)

7) Zhou, C., Chen, Y., Yang, Z., & Khoshnevis, B. Development of a Multi-material Mask-Image-Projection-based Stereolithography for the Fabrication of Digital Materials. *Proc Solid Freeform Fabr.* Austin, TX, 65-80 (2011).

8) Peterson, G. I. *et al.* Production of Materials with Spatially-Controlled Crosslink Density via Vat Photopolymerization. *Appl. Mater. Interfaces* (2016). doi:10.1021/acsami.6b09768

9) Huang, Y., Leu, M. C,. Mazumder, J., & Donmez, A. Additive Manufacturing: Current State, Future Potential, Gaps and Needs, and Recommendations. *Journal of Manufacturing Science and Engineering* **137**, 014001 (2015).

10) Espalin, D., Ramirez, J. A., Medina, F., & Wicker, R. Multi-material, multi-technology FDM: exploring build process variations. *Rapid Prototyping Journal* **20**, 3, 236-244 (2014).

11) Stratasys J750. Stratasys Ltd. Available at http://www.stratasys.com/3d-printers/production-series/stratasys-j750. (accessed 21 Sept 2016)

12) Projet MJP 2500 Series. 3D Systems, Inc. Available at http://www.3dsystems.com/3d-printers/professional/projet-mjp-2500-series. (accessed 21 Sept 2016)

13) De Gans, B. J., Duineveld, P. C., & Schubert, U. S. Inkjet printing of polymers: state of the art and future developments. *Advanced Materials* **16**, 203-213 (2004).

14) Meisel, N., & Williams, C. An Investigation of Key Design for Additive Manufacturing Constraints in Multimaterial Three-Dimensional Printing. *Journal of Mechanical Design* **137**, 111406 (2015).

15) Park, Y. J., Lim, D. H., Kim, H. J.; Park, D. S., & Sung, I. K. UV- and thermal-curing behaviors of dual-curable adhesives based on epoxy acrylate oligomers. *International*

Journal of Adhesion and Adhesives **29**, 7, 710-717 (2009).

16) Moussa, K. & Decker, C. Kinetic study of the cationic photopolymerization of epoxy monomers. *Polym. Chem.* **28**, 12, 3429-3443 (1990).

17) Corcione, C. E., Greco, A., & Maffezzoli, A. Photopolymerization kinetics of an epoxy-based resin for stereolithography. *J. Appl. Pol. Sci.* **92**, 6, 3484-3491 (2004).

18) Crivello, J. V. Benzophenothiazine and benzophenoxazine photosensitizers for triarylsulfonium salt cationic photoinitiators. *Poly. Chem.* **46**, 11, 3820-3829 (2008).

19) Crivello, J. V. & Sangermano, M. Visible and long-wavelength photoinitiated cationic polymerization. *Polym. Chem.* **39**, 3, 343-356 (2001).

20) Durmaz, Y. Y., Moszner, N., & Yagei, Y. Visible Light Initiated Free Radical Promoted Cationic Polymerization Using Acylgermane Based Photoinitiator in the Presence of Onium Salts. *Macromolecules* **41**, 6714-6718 (2008).

21) Wang, Tao., Chen, J. W., Li, Z. Q., & Wan, P. Y. Several ferrocenium salts as efficient photoinitiators and thermal initiators for cationic epoxy polymerization. *Journal of Photochemistry and Photobiology A* **187**, 389-394 (2007).

22) Zhang, J. *et al.* Cationic Photoinitiators for Near UV and Visible LEDs: A Particular Insight into One-Component Systems. *Macromolecular Chemistry and Physics* **217**, 1214-1227 (2016).

23) Robeson, Lloyd. Samulski, Edward. Ermoshkin, Alexander. Desimone, Joseph. Continuous three dimensional fabrication from immiscible liquids. U.S. Patent Office 026613 (2014).

Chapter 3. Modular Elastomer Photoresins for Vat Photopolymerization

3.1. Introduction

Additive manufacturing (AM), such as 3D printing, has experienced explosive growth at the interface of chemistry and engineering.[1–6] Recent breakthroughs have generated exciting opportunities to print a broad range of object geometries with impressive throughput.[7–9] As printer capabilities have rapidly evolved, the technologies for expanding the scope of build materials has started to follow suit. Innovations in synthetic macromolecular chemistry and nano-to-mesoscale molecular design have been vetted against, inspired by, and integrated with cutting-edge AM equipment to produce unprecedented outcomes in multiple fields.[10–15] A challenging and potentially highly rewarding target area for new materials development lies within elastomeric systems that display rapid customizability in molecular composition, to complement rapid prototyping available from AM.

Integration of elastomers with AM technology offers exciting potential capabilities for multiple areas, including soft robotics, flexible electronics, biomimetic structures, and wearable devices.[6,11,13,14,16–23] Many current fabrication processes that incorporate elastomer materials into devices involve tedious and time-consuming iterative processing or assembly steps.[17,18] AM, on

*Large portions of this chapter have been submitted for publication in Thrasher, C. J.; Schwartz, J. J.; Boydston, A. J. *Adv. Func. Mat.* **2017**

the other hand, can be a facile method to quickly fabricate complex 3D geometries in a single process. Among the various AM techniques available, digital light processing additive manufacturing (DLP-AM) is particularly attractive as it can offer a low equipment cost option, high resolution print features, and relatively fast print speeds while enabling access to hollow object components, overhangs, and other challenging geometries.[24] Recent advancements in DLP-AM show precision control over architectures with sub-micrometer resolution, 3D spatial control over cross-linking density, and continuous printing able to produce 10 cm objects in minutes.[7–9,25]

Options for using DLP-AM to print stretchable devices are currently restricted by a lack of printable flexible materials, but recent advances have begun to answer this call.[11,10,12] Commercially available "flexible" photoresins such as Formlabs Flexible and Spot-E Elastic exhibit limited elongations from 90-100%, which is not sufficient for many advanced applications.[26,27] Another impressive photoresin, Carbon's Flexible Polyurethane resin, shows high mechanical toughness and elongations up to 300%, but are not yet available on open platforms.[28] Magdassi and Ge recently demonstrated UV-curing and AM of resins to produce objects capable of tensile strains of 270%.[10] Other promising resins in their study displayed strains of up to 1100%, although their 3D printability may be limited by their high viscosity. Commercial elastomer (or flexible) photoresins are often proprietary, challenging to modify, and require extra equipment to achieve desired printing characteristics (e.g., custom heating elements to combat high viscosities). Therefore, more diverse resin formulations and basic tools to enable elastomer 3D printing are needed.

3.2. Methods

bis(propylacrylamide)poly(dimethylsiloxane) (PDMSDMAA). Methacryloyl chloride (22 mmol) was added dropwise into a solution of bis(propylamine)poly(dimethylsiloxane) (10

mmol) and anhydrous triethylamine (22 mmol) in CH_2Cl_2 (150 mL) at 0 °C. The reaction mixture was then stirred for 24 h, during which time the ice batch expired. The CH_2Cl_2 was then removed under reduced pressure, and then hexanes (200 mL) was added to the reaction mixture. The solution was then filtered through a fitted glass frit. The filtrate was then washed with an 80/20 mixture of brine and saturated aqueous sodium bicarbonate solution (3 × 100 mL). A centrifuge was used to separate the emulsion when necessary. The organic phase was subsequently dried with anhydrous calcium sulfate, filtered, and concentrated under reduced pressure to yield a viscous clear liquid (83% yield). ^{1}H NMR (500 MHz, $CDCl_3$, 298 K, δ, ppm): 5.85 (s, 1H), 5.67 (s, 1H), 5.30 (s, 1H), 3.30 (q, J = 6.5 Hz, 2H), 1.96 (s, 3H), 1.56 (m, J = 8 Hz, 2H), 0.55 (m, J = 4.5 Hz, 2H), 0.07 (s, 198H).

Monomer Leaching. Printed disks (r = 10 mm, h = 1 mm) of each material were weighed and then soaked in 3.0 mL of CH_2Cl_2 for 2 h. A separate vial was then filled with 1.0 mL of the 3.0 mL of soaking solution. These solutions were analyzed by GC/MS and the abundance of peaks corresponding to HEA and EEEA were recorded. GC/MS was accomplished with injection volumes of 1 μL, an initial oven temp of 60 °C held for 1 min, ramped 15 °C/min to 320 °C and held for 3 min. HEA monomer was found at t = 4.143 min and EEEA monomer was found at 7.434 min. A stock solution of 0.1 mg/mL HEA and EEEA was prepared and the abundance of peaks corresponding to HEA and EEEA were recorded and used to correlate abundance and concentration. Mass of monomer leeched was determined using the converted concentration and 3.0 mL of total starting solution and subsequently compared to the mass of the respective printed disk.

Characterization. ^{1}H NMR spectra were recorded on a Bruker AVance 500 MHz spectrometer. Chemical shifts are reported in delta (δ) units, expressed in parts per million (ppm) downfield

from tetramethylsilane using the residual protio-solvent as an internal standard (CDCl3, 1H: 7.26 ppm). Tensile elongation was conducted according to ASTM D638 using type V specimen samples. Testing was accomplished with an Instron 5585H Universal Testing System equipped with a 50 N load frame, pneumatic grips, and Bluehill 3 software. Elongation was conducted at a 100 mm/min extension rate and an Instron 2663-821 Advanced Video Extensometer was used to track strain. Light intensity of projectors used for vat photopolymerization was measured using an Extech Instruments light meter (model HD450). Durometer measurements were taken in triplicate and reported as averages using a PCE Instruments PCE-DD-A Shore A Durometer. Rheology measurements were taken on a TA Instruments Discovery HR-2 hybrid rheometer using a stainless steel 20 mm Peltier plate. Data was collected from a strain sweep test from 10 - 50,000 Pa at 25 °C and an angular frequency of 6.28 rad/s. Storage and loss modulus data were compared near 0.1 % oscillation strain. GC/MS measurements were accomplished with a combined Hewlett Packard 5973 Mass Selective Detector and HP 6890 Series GC System using an Agilent 7683 Series Injector. Shore A hardness was determined using a PCE-DD-A durometer.

3D Printing. Objects were printed using a SeeMeCNC Droplit DLP 3D Printer and an Acer X1161P projector. The multi-material gripper, gyroid lattice, and octet truss were printed using an Optoma HD20 with the UV filter removed and the brightness decreased to 40% (via projector menu). Creation Workshop (version 1.0.0.75) software was used to operate/control the printer and projector as well as convert 3D model files (STL format) constructed using Google Sketchup (version 17.1.174) into image stacks for printing. The build vat consisted of a Pyrex Petri-dish (d = 90 mm) with a layer of silicon elastomer (ca. 11 g of silicon applied to dish). Prints were conducted by repeating the process of projecting an image into the resin followed by raising the

z-stage (Figure 2.2). Post-print parts were subjected to an excess of white light at printing intensity for 30 seconds per side. Multi-material printing and individual printer settings for each photoresin are described in the supplementary information.

3.3. Results and Discussion

In our studies, we found 2-hydroxyethyl acrylate (HEA) to be an advantageous resin component for DLP-AM. HEA benefits from hydrogen bonding, which has been reported previously to suppress the termination rate of radical polymerization.[50] This rapid polymerization helps to counter the deleterious effects of termination events from oxygen in ambient air. Hydroxyalkyl acrylates can also undergo a chain transfer mechanism involving hydrogen atom abstraction alpha to the hydroxyl group, leaving a carbon centered radical that can reinitiate and create a cross-linking event.[51] In practice, this chain-transfer mechanism yields a light cross-linking effect during photopolymerizations of HEA that adds structural stability. Hydrogen bonding in poly(HEA) also facilitates printing by yielding solid layers at lower conversions, which can correspond to shorter cure times, in comparison with non-hydrogen bonding resins. In the printed objects, hydrogen bonding also provides structural stability under strain leading to the high elongations at break of these materials. In this manner, the hydrogen bonds dynamically break and reform, dissipating energy as the material is deformed.

Desirable characteristics for AM with photoresins include resilience to ambient atmosphere, short cure times for each layer, and low viscosities. The features of many bulk photopolymerizations therefore make adaptation for DLP-AM non-trivial.[5] A series of elastomer photoresin compositions compatible with DLP-AM that yield soft, flexible, and elastic materials are reported herein. The resin formulations (Table 3.1) enable access to a range of polarities, spanning hydrogel to silicone elastomer materials, and result in objects of varied composition,

mechanical properties, and swelling behaviors. Moreover, all printing was performed with low-cost entry-level projector and printer equipment, which included visible light DLP without temperature regulation of the vat. For each photoresin, a certain amount of photoinitiator Irgacure 819 was added. Irgacure 819 was chosen for its high reactivity, absorption in visible light, low cost, and low cytotoxicity.[29] To denote the amount of Irgacure 819 photoinitiator used in a particular photoresin, the wt% with respect to monomer or parts per hundred rubber (phr) is written in parenthesis after the name of the resin. For example, ThrashOHflex (1) refers to ThrashOHflex with 1 phr of Irgacure 819.

Drawing inspiration from their materials properties and widespread utility, silicone-based elastomers were an initial target. Representative thermally-cured examples include tough and flexible specimens produced from Dragon Skin 30 (364% elongation at break) and Sylgard 184 (140% elongation at break).[30,31] To enable DLP-AM, a polydimethylsiloxane dimethacrylamide (PDMSDMAA) oligomer having M_n = 3.0 kDa based upon ^{1}H NMR analysis was prepared. Initial prints were thwarted by the fact that the PDMSDMAA swelled into the silicone lining of the vat. Attempts to print using an uncoated glass surface were hindered by strong adhesion of the cured layers to the glass, causing detachment of the print object from the rising build stage. Previous studies have avoided these issues by using a PTFE-lined vat.[32] It was found that printing with a biphasic liquid vat system was successful (see Chapter 2.3).[33] Specifically, the PDMSDMAA photoresin was layered on top of a solution of brine. The build stage was then positioned just above the liquid-liquid interface, which defined the upper and lower boundaries of the build layer, respectively. Printing of successive layers was found to proceed smoothly and give rise to optically transparent elastomeric specimens (Figure 3.1).

Moving toward increasingly polar and hydrophilic resin materials, combinations of PDMSDMAA with common acrylate-based resin materials were evaluated. In particular, it was found that PDMSDMAA could be formulated with 2-hydroxyethyl acrylate (HEA) and butyl acrylate (BA) using cetrimonium bromide surfactant. This photoresin, referred to as SilOHflex (Table 3.1), offered convenient printing properties and signifies a broad scope of resin component classes that can be used to tune the materials properties of the printed objects. Having observed promising printability from this HEA-based mixture, an opportunity to move toward resin formulations that would give rise to hydrogel products upon DLP-AM was noted.[34–39] We found that combinations of HEA with 2-(2-ethoxyethoxy)ethyl acrylate (EEEA) also yielded a promising elastomer resin (ThrashOHflex). Finally, DLP-AM with HEA (referred to here as HydrOHflex) was investigated and good printability yielding clear hydrogel materials was observed.

The resin compositions we evaluated herein were found to be remarkably printable. As low viscosity liquids, they can be printed at room temperature and we achieved relatively short layer cure times times (6 – 15 s). The resins are optically clear and can be printed with no dye added, although it is noted that addition of dyes does appear to improve resolution. Specifically, when printing hollow structures and unsupported crossbeams the addition of dyes is recommended. The standard post-cure procedure, which involved approximately 3 min of illumination with white light, seemed effective at increasing conversion and fixing the final structures (Table 3.2). The extent of curing was found to generally exceed 99%, given that less than 10 mg of uncured resin was extracted per gram of solid printed material during leaching tests with a good swelling solvent.

Representative examples of printed objects are depicted in Figure 3.1. A qualitative assessment of the optical clarity of each resin can be made from the overlay with printed text (Figure 3.1A). As can be seen in the ThrashOHflex series, increasing the feed ratio of Irgacure 819 resulted in slightly increased coloration of the final object. SilOHflex also stood out as offering less clarity, is speculated to arise from the greater disparity in resin component properties and potential microphase separation in comparison with the other resins. In addition to simple test specimen geometries, more advanced structures were also easily obtained. Figure 3.1B depicts an octet truss unit cell printed from SilOHflex, and Figure 3.1C shows a gyroid lattice from HydrOHflex. In general, each of the resins we evaluated were successful in printing each of our attempted geometries.

Test specimens printed from each photoresin formulation were evaluated by tensile testing, rheology, durometry, and swelling experiments. Notably, effects of initiator concentration were not exhaustively explored; however, we did see discernable differences in layer cure time, extension to break, moduli, and color for ThrashOHflex, an intermediate polarity resin within our series. Specifically, ThrashOHflex with photoinitiator amounts of 0.25, 1, and 2 phr were evaluated, which are within the initiator concentration range typically used in vat photopolymerization. Representative data are depicted in Figure 3.2 and summarized in Table 3.3.

Shore A hardness values ranged from 5 – 25 (Table 3.3) and were tunable within this range. For comparison, ThrashOHflex resins have hardness values comparable to human skin[42] whereas SilOHflex, HydrOHflex, and PDMSDMAA are similar to a solid rubber ball.[43] Tensile testing (Figure 3.2A) revealed a relatively low elongation to break for the PDMSDMAA materials (51%), leaving considerable room for improvement with respect to thermally cured

silicone elastomers. In contrast, the other photoresin formulations produced test samples showing 247 – 348% maximum strains. Maximum strain and tensile strength were found to be sensitive to the amount of photoinitiator used (cf. ThrashOHflex with 0.25, 1, and 2 phr Irgacure 819), although clear correlations were not apparent.

Each of the resins appeared to result in elastomeric printed specimens based upon repeated tensile loading. Representative quantitative data for HydrOHflex is depicted in Figure 3.2B. The results show very little hysteresis and no sign of creep or fatigue after 5 cycles, indicating a highly recoverable elastic response. This is relevant for soft robotics and wearable devices where it is desirable to have controlled and repeatable deformation at high frequency.[17,23,36,44] Notably, this rapid recoverability is distinct from many other hydrogen bonding materials, which often require a delayed "reset" period to allow for re-equilibration and obtain full property recovery.[10,34,38,39] Consistent with cyclic tensile loading and qualitative macroscopic behavior, rheological experiments revealed G' to be greater than G" for each material (Table 3.3). Moreover, tan δ values (a measure of energy dissipation efficiency) spanned one order of magnitude, from 0.04 to 0.51, signifying broad tunability of elastic response.

The effects of printing orientation on tensile stress-strain behavior were also evaluated. Most AM methods produce objects with anisotropic properties dependent upon the print orientation used during fabrication.[45,46] For example, differences in materials properties can emerge from incomplete interdigitation between layers during printing processes. Achieving uniform properties throughout complex geometries is an area in which AM tends to underperform when compared to traditional manufacturing methods. ThrashOHflex (1) was chosen as a representative resin of both middling polarity and photoinitiator concentration to

evaluate the effects of layering during DLP-AM (Figure 2C). It was found that the tensile characteristics of printed dogbones of ThrashOHflex (1) were largely independent of printing orientation. Of particular note, samples printed in the ZX orientation with layers perpendicular to the axis of elongation displayed similar stress-strain behavior as those printed in the XY and XZ orientations. This suggests that newly formed layers were not completely cured and were capable of absorbing additional resin. In this way, interdigitation could be achieved by across layers.

The disparate hydrophilicities of the resin materials suggested that the resulting printed objects would display varied swelling behavior. To investigate, 10-layer discs (r = 10 mm, h = 1 mm) were printed and their swelling characteristics in water recorded (Table 3.4). As expected, the silicone-containing resins displayed the least volumetric change, with PDMSDMAA-based specimens showing essentially no swelling ($\Delta V = 1.01$). ThrashOHflex and HydrOHflex each showed considerably higher values of ΔV upon swelling. Interestingly, ThrashOHflex had the highest ΔV value in the series, whereas HydrOHflex had the greatest increase in mass. The disparate densities of the two materials may be attributed to the greater presence of hydrogen bonding in HydrOHflex, however, it is emphasized that printing conditions and crosslink densities are also likely to impact the swelling behavior of the printed products.

To demonstrate the utility of these resins for DLP-AM, a three-armed multi-material pneumatic gripper was designed and printed as a single part (Figure 3). The gripper incorporated several design parameters previously demonstrated through the construction of multi-part soft-robots.[47,48] More specifically, the differential strain between a highly flexible layer (purple) and a flexible but higher modulus “strain limiting” layer (gold) as well as the incorporation of top walls were employed to enhance actuation efficiency. Furthermore, hard talons made from a hexane-1,6-diol diacrylate/HEA mixture were incorporated to take advantage of soft-to-hard

material transitions that have proven beneficial in other systems.[22,49–51] The pneumatically driven bending motion and gripping capabilities are depicted in Figure 3.3.

3.4. Conclusion

New elastomer photoresins with high elongation suitable for use in 3D printing technologies such as vat photopolymerization and photo-jetting were presented. These resins are derived from readily available feedstocks and accessible with minimal synthetic outlay. The photoresins are low viscosity, optically transparent, and printable on open platforms without the use of custom equipment. As demonstrated herein, DLP-AM can easily fabricate these resins into complex object geometries, such as lattice structures and a functional soft robotic gripper. Furthermore, variations in composition enable modular and tunable materials properties to include mechanical and swelling characteristics. These resin formulations may find utility in their current iterations, but more importantly, they can also serve as a platform for facile customization based on a molecular-level understanding of the chemistry involved.

Table 3.1. Compositions of Photoresins Studied.

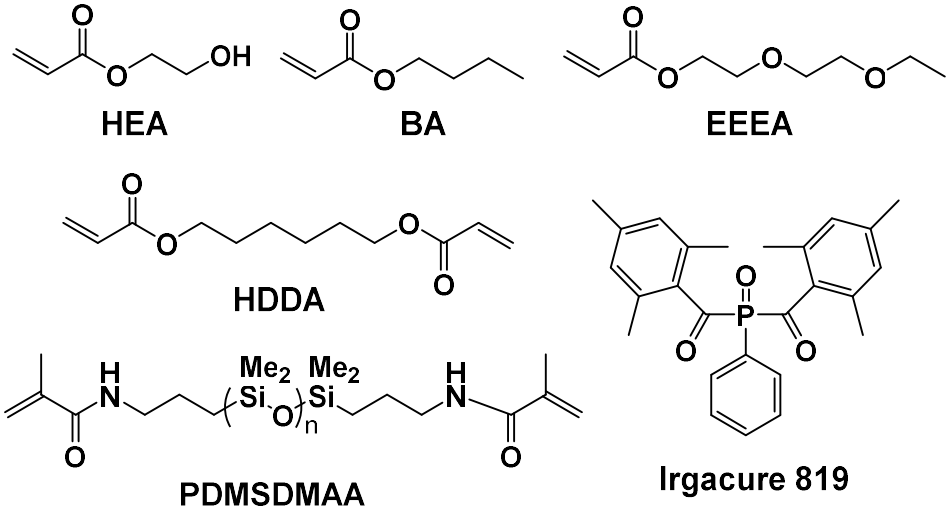

photoresin	resin composition (by weight)
PDMSDMAA	PDMSDMAA (95%), toluene (5%), Irgacure 819 (0.25 phr)
SilOHflex	HEA (64%) , BA (27%), PDMSDMAA (9%), Irgacure 819 (0.25 phr), cetrimonium bromide (0.25 phr)
ThrashOHflex	EEEA (60%), HEA (40%), Irgacure 819 (0.25, 1, or 2 phr)
HydrOHflex	HEA(100%), Irgacure 819 (1 phr)

Table 3.2. Results of Leaching Studies. Quantification of extractable monomer after printing for each photoresin composition, measured in milligrams of extracted monomer per gram of printed polymer.

Photoresin	HEA (mg/g)	EEEA (mg/g)
SilOHflex (0.25)	1.136 ± 0.034	N.A.
ThrashOHflex (0.25)	0.387 ± 0.018	7.709 ± 0.238
ThrashOHflex (0.25) no post-cure	2.145 ± 0.041	24.244 ± 1.050
ThrashOHflex (1)	0.003 ± 0.000(1)	0.288 ± 0.010
ThrashOHflex (2)	0.129 ± 0.008	3.511 ± 0.178
HydrOHflex (1)	0.020 ± 0.002	N.A.

Table 3.3. Summary of properties determined by tensile elongation, rheology, and durometry.[a]

material	σ_{max} (MPa)[c]	ε_{max}[d]	Shore A hardness	G' (MPa)[e]	G'' (MPa)[f]	tan δ[g]
PDMSDMAA (0.25)	0.58 ± 0.09	0.51 ± 0.06	23.0 ± 2.0	1.74 ± 0.22	0.07 ± 0.01	0.04 ± 0.02
SilOHflex (0.25)[b]	1.01 ± 0.03	3.38 ± 0.08	22.0 ± 1.0	2.28 ± 0.47	1.17 ± 0.29	0.51 ± 0.002
ThrashOHflex (0.25)	0.44 ± 0.08	3.26 ± 0.50	6.5 ± 1.0	0.81 ± 0.31	0.12 ± 0.05	0.15 ± 0.01
ThrashOHflex (1)	0.30 ± 0.02	2.47 ± 0.23	5.8 ± 0.8	0.97 ± 0.13	0.17 ± 0.01	0.18 ± 0.01
ThrashOHflex (2)	0.29 ± 0.26	3.28 ± 0.32	5.0 ± 0.5	0.76 ± 0.24	0.15 ± 0.05	0.20 ± 0.02
HydrOHflex (1)	1.23 ± 0.31	3.48 ± 0.26	18.8 ± 0.8	2.18 ± 0.21	1.06 ± 0.14	0.49 ± 0.03

[a] Values are averages of three trials and standard deviations are reported.
[b] Samples were prone to slip out of the pneumatic grips used during tensile testing before failing due to strain. The strain at slippage was used to approximate the strain at break for these samples and is therefore likely to be an underestimated value.
[c] σ_{max} is the ultimate tensile strength determined from ASTM D638 testing.
[d] ε_{max} is the elongation at break determined from ASTM D638 testing.
[e] G' is the storage modulus determined by rheology.
[f] G'' is the loss modulus determined by rheology.
[g] tan δ = G''/G'.

Table 3.4. Results of Swelling Experiments. Swelling behavior for printed discs with radius = 10 mm and height = 1 mm. Specimens were submerged in deionized water for 24 h, and then removed and patted dry. All values are an average of three trials, errors = 1 standard deviation. [b] Masses were recorded on an analytical balance. [c]Volumes were calculated based upon dimensions measured using a digital caliper.

material	mass increase[b]	volume increase[c]
PDMSDMAA (0.25)	1.01 ± 0.01	1.01 ± 0.01
SilOHflex (0.25)	1.55 ± 0.06	1.64 ± 0.20
ThrashOHflex (1)	2.49 ± 0.06	3.25 ± 0.75
ThrashOHflex (2)	2.50 ± 0.03	3.25 ± 0.25
ThrashOHflex (0.25)	2.70 ± 0.01	3.38 ± 0.28
HydrOHflex (1)	3.35 ± 0.07	2.84 ± 0.73

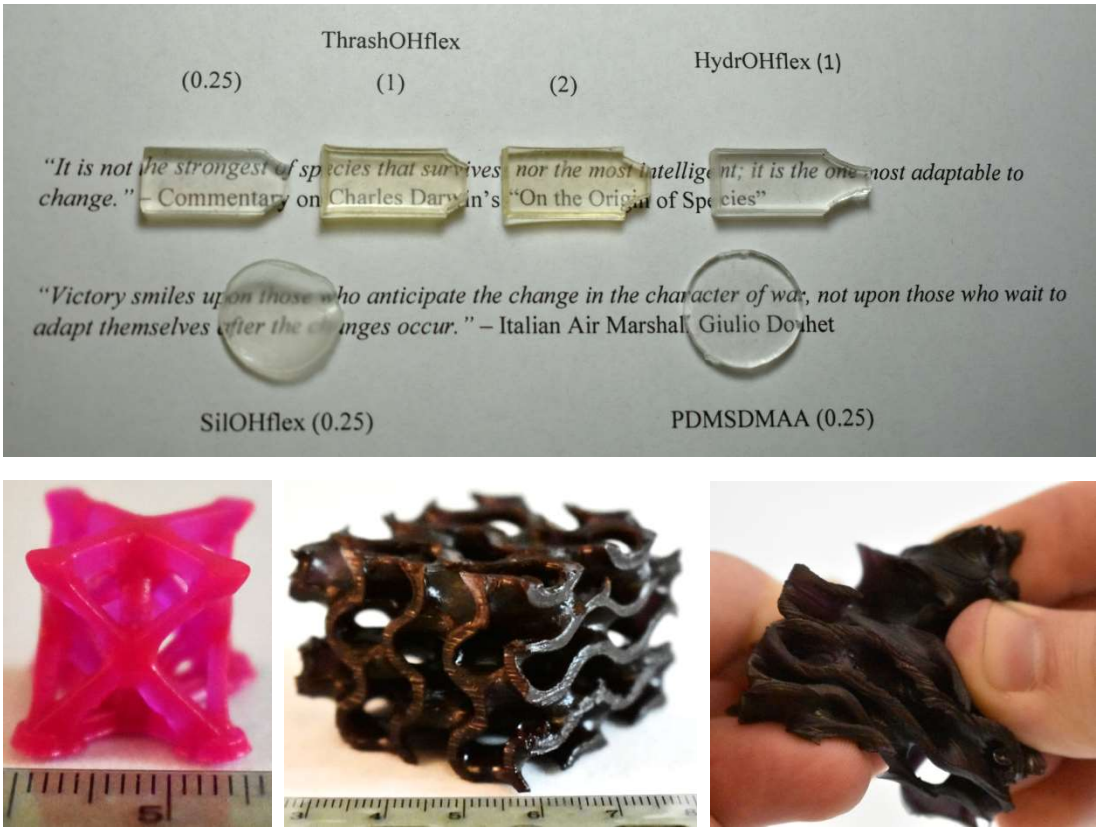

Figure 3.1. Photos of Printed Objects. A) Printed objects of different resin compositions overlaid on printed text (font = Times New Roman 11 pt). Numbers in parentheses indicate phr of Irgacure 819 in the feed. B) Octet truss unit cell printed from SilOHflex, ruler units = cm, cell dimensions = 1.5 × 1.5 × 1.5 cm^3, print time = 31 min. C) Gyroid lattice printed from HydrOHflex, ruler units = cm, lattice dimensions = 4 × 4 × 3 cm^3, print time = 49 min.

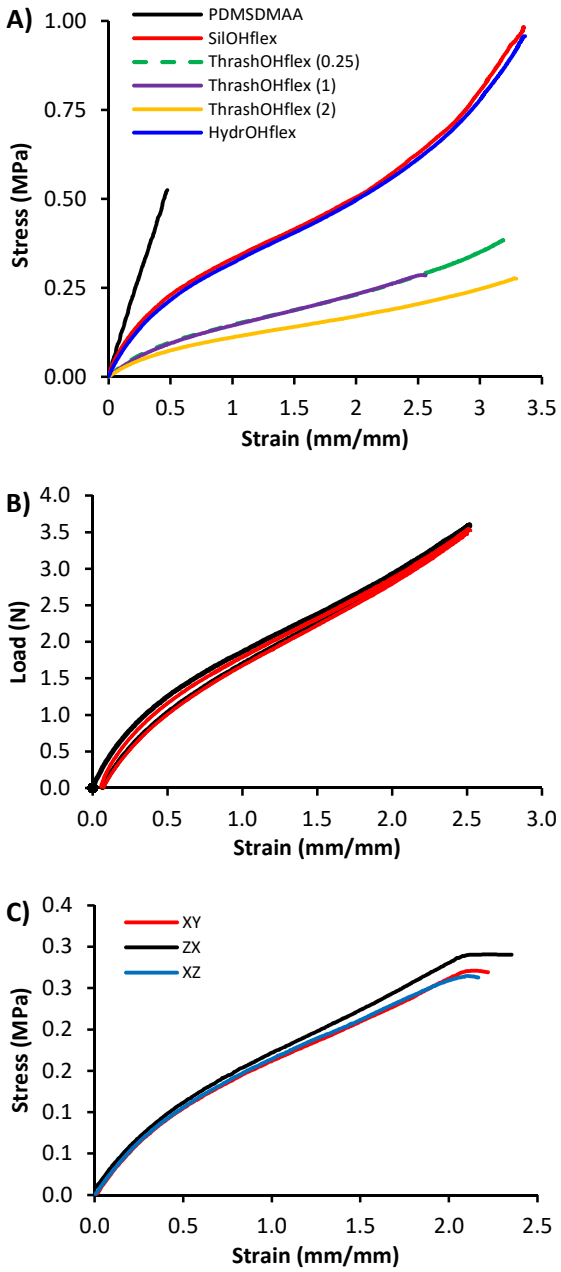

Figure 3.2. Tensile Testing of Elastomer Materials. Tensile test results for printed specimens (ASTM D638 Type V dogbones: A) Comparison of stress-strain curves from various photoresin compositions. B) Cyclic tensile elongation (total cycles = 5) of HydrOHflex (1). Specimens were elongated at 100 mm/min to 250% strain. The first cycle is shown in black and cycles 2 – 5 are shown in red. C) Comparison of stress-strain curves from tensile elongation of specimens of ThrashOHflex (1) printed in the XY, XZ, and ZX orientations.

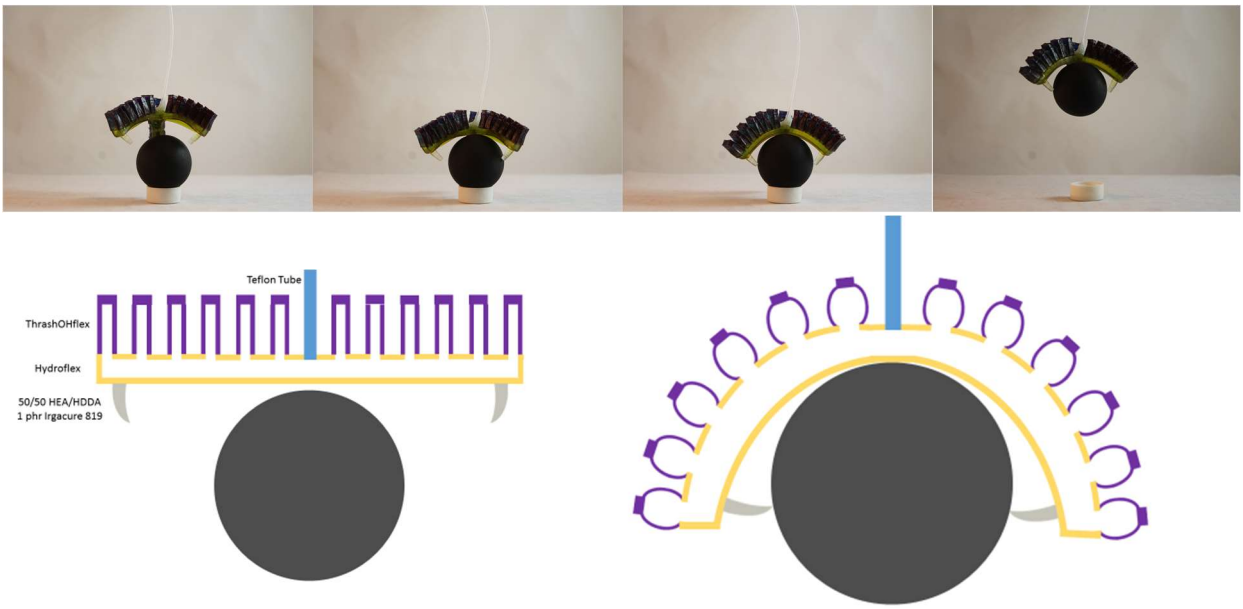

Figure 3.3. Actuation of 3D Printed Multi-material Pneumatic Gripper A) Gripper descending, pneumatically actuating, and lifting a plastic ball. Ball mass = 2.6 g. B) Idealized cross-sectional illustration of gripper before (top) and after (bottom) pneumatic actuation.

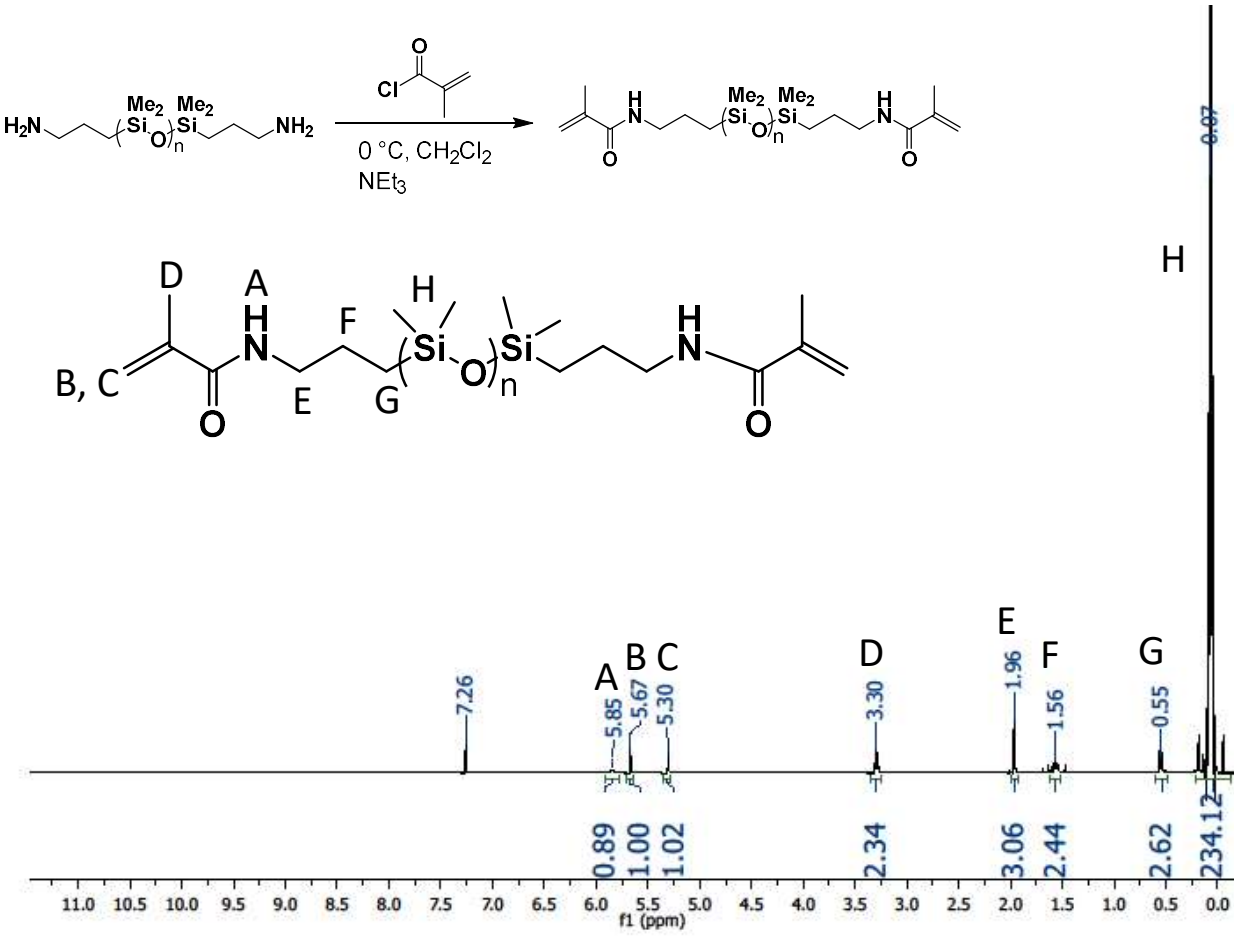

Figure 3.4. ^{1}H NMR and Synthetic Scheme of bis(propylacrylamide)poly(dimethylsiloxane). ^{1}H NMR was taken in in $CDCl_3$. End group analysis shows M_n = 3.0 kDa. Yield of reaction was 83%.

Notes to Chapter 3

1. Gross, B. C., Erkal, J. L., Lockwood, S. Y., Chen, C. & Spence, D. M. Evaluation of 3D Printing and Its Potential Impact on Biotechnology and the Chemical Sciences. *Anal. Chem.* **86,** 3240–3253 (2014).
2. Gross, B., Lockwood, S. Y. & Spence, D. M. Recent Advances in Analytical Chemistry by 3D Printing. *Anal. Chem.* **89,** 57–70 (2016).
3. Melchels, F. P. W., Feijen, J. & Grijpma, D. W. A review on stereolithography and its applications in biomedical engineering. *Biomaterials* **31,** 6121–6130 (2010).
4. Melchels, F. P. W. *et al.* Additive manufacturing of tissues and organs. *Prog. Polym. Sci.* **37,** 1079–1104 (2012).
5. Stansbury, J. W. & Idacavage, M. J. 3D printing with polymers: Challenges among expanding options and opportunities. *Dent. Mater.* **32,** 54–64 (2016).
6. Leu, M. C. & Arbor, A. Additive Manufacturing: Current State, Future Potential, Gaps and Needs, and Recommendations. *J. Manuf. Sci. Eng.* **137,** 1–10 (2016).
7. Tumbleston, J. R. *et al.* Continuous liquid interface production of 3D objects. *Science* **347,** 635–639 (2008).
8. Sun, C., Fang, N., Wu, D. M. & Zhang, X. Projection micro-stereolithography using digital micro-mirror dynamic mask. *Sensors Actuators A* **121,** 113–120 (2005).
9. Zheng, X. *et al.* Design and optimization of a light-emitting diode projection micro-stereolithography three-dimensional manufacturing system. *Rev. Sci. Instrum.* **83,** (2015).
10. Patel, D. K., Sakhaei, A. H., Layani, M., Ge, Q. & Magdassi, S. Highly Stretchable and UV Curable Elastomers for Digital Light Processing Based 3D Printing. *Adv. Mater.* (2017). doi:10.1002/adma.201606000
11. Zarek, M. *et al.* 3D Printing of Shape Memory Polymers for Flexible Electronic Devices. *Adv. Mater.* **28,** 4449–4454 (2016).
12. Ge, Q. *et al.* Multimaterial 4D Printing with Tailorable Shape Memory Polymers. *Sci. Rep.* **6,** 31110 (2016).
13. Wu, W., Deconinck, A. & Lewis, J. A. Omnidirectional Printing of 3D Microvascular Networks. *Adv. Healthc. Mater.* 178–183 (2011). doi:10.1002/adma.201004625
14. Truby, R. L. & Lewis, J. A. Printing soft matter in three dimensions. *Nature* **540,** 371–378 (2016).
15. Mannoor, M. S. *et al.* 3D printed bionic ears. *Nano Lett.* **13,** 2634–2639 (2013).
16. Kim, S., Laschi, C. & Trimmer, B. Soft robotics: a bioinspired evolution in robotics. *Trends Biotechnol.* **31,** 287–294 (2013).
17. Hines, L., Petersen, K., Lum, G. Z. & Sitti, M. Soft Actuators for Small-Scale Robotics. *Adv. Mater.* (2017). doi:10.1002/adma.201603483

18. Zolfagharian, A. *et al.* Physical Evolution of 3D printed soft actuators. *Sensors Actuators A. Phys.* **250,** 258–272 (2016).

19. Rogers, J. A., Someya, T. & Huang, Y. Materials and Mechanics for Stretchable Electronics. *Science* **327,** 1603–1607 (2010).

20. Bartlett, N. W. *et al.* robot powered by combustion. *Science* **349,** 161–165 (2015).

21. Sekitani, T. *et al.* diode display using printable elastic conductors. *Nat. Mater.* **8,** 494–499 (2009).

22. Wegst, U. G. K. *et al.* Bioinspired structural materials. *Nat. Mater.* **14,** 23–36 (2014).

23. Muth, J. T. *et al.* Embedded 3D Printing of Strain Sensors within Highly Stretchable Elastomers. *Adv. Mater.* 6307–6312 (2014). doi:10.1002/adma.201400334

24. Zheng, X. *et al.* Ultralight, Ultrastiff Mechanical Metamaterials. *Science* **344,** 1373–1377 (2014).

25. Peterson, G. I. *et al.* Production of Materials with Spatially-Controlled Crosslink Density via Vat Photopolymerization. *Appl. Mater. Interfaces* (2016). doi:10.1021/acsami.6b09768

26. Spot A Materials. Spot-E Elastic. Available at: http://spotamaterials.com/product/spot-e-1kg/ (Accessed March 2017)

27. Formlabs. Formlabs Flexible. (2017). Available at: https://formlabs.com/materials/engineering/#flexible. (Accessed March 2017)

28. Carbon3D. FPU Flexible Polyurethane. Available at: http://www.carbon3d.com/materials/fpu-flexible-polyurethane. (Accessed March 2017)

29. Schuster, M. *et al.* Evaluation of Biocompatible Photopolymers I: Photoreactivity and Mechanical Properties of Reactive Diluents. *J. Macromol. Sci. Part A* **44,** 547–557 (2007).

30. Smooth-On. Dragon Skin 30. Available at: https://www.smooth-on.com/products/dragon-skin-30/. (Accessed February 2017)

31. Dow Corning. Sylgard 184. Available at: http://www.dowcorning.com/applications/search/products/Details.aspx?prod=01064291. (Accessed February 2017)

32. Eckel, Z. C. *et al.* Additive manufacturing of polymer-derived ceramics. *Science* **351,** 58–62 (2015).

33. Robeson, Lloyd. Samulski, Edward. Ermoshkin, Alexander. Desimone, Joseph. Continuous three dimensional fabrication from immiscible liquids. U.S. Patent Office 026613 (2014).

34. Liu, J. *et al.* Biomimetic Supramolecular Polymer Networks Exhibiting both Toughness and Self-Recovery. *Adv. Mater.* (2017). doi:10.1002/adma.201604951

35. Liqi Si, Xiaowen Zheng, Jun Nie, Ruixue Yin, Y. H. and X. Z. Silicone-based tough hydrogels with high resilience, fast self-recovery, and self-healing properties. *Chem.*

Commun. **52,** 8365–8368 (2016).

36. Duan, J., Liang, X., Guo, J., Zhu, K. & Zhang, L. Ultra-Stretchable and Force-Sensitive Hydrogels Reinforced with Chitosan Microspheres Embedded in Polymer Networks. *Adv. Mater.* **28,** 8037–8044 (2016).

37. Jeon, I., Cui, J., Illeperuma, W. R. K., Aizenberg, J. & Vlassak, J. J. Extremely Stretchable and Fast Self-Healing Hydrogels. *Adv. Mater.* **28,** 4678–4683 (2016).

38. Liu, J. *et al.* Bioinspired Engineering of Two Different Types of Sacrificial Bonds into Chemically Cross-Linked cis-1,4-Polyisoprene toward a High-Performance Elastomer. *Macromolecules* (2016). doi:10.1021/acs.macromol.6b01576

39. Reinecke, A., Bertinetti, L., Fratzl, P. & Harrington, M. J. Cooperative behavior of a sacrificial bond network and elastic framework in providing self-healing capacity in mussel byssal threads. *J. Struct. Biol.* (2016). doi:10.1016/j.jsb.2016.07.020

40. Kissin, E. Y. *et al.* Durometry for the assessment of skin disease in systemic sclerosis. *Arthritis Rheum.* **55,** 603–9 (2006).

41. Mykin Inc. Rubber Hardness Chart. Available at: http://mykin.com/rubber-hardness-chart. (Accessed: 1st February 2017)

42. Rossiter, J., Walters, P. & Stoimenov, B. Printing 3D dielectric elastomer actuators for soft robotics. *Proc. SPIE* **7287,** (2009).

43. Farzadi, A., Solati-hashjin, M., Asadi-eydivand, M., Azuan, N. & Osman, A. Effect of Layer Thickness and Printing Orientation on Mechanical Properties and Dimensional Accuracy of 3D Printed Porous Samples for Bone Tissue Engineering. *PLoS One* **9,** 1–14 (2014).

44. Carbon3D. Carbon3D Materials. Available at: http://www.carbon3d.com/materials. (Accessed March 2017)

45. Ilievski, F., Mazzeo, A. D., Shepherd, R. F., Chen, X. & Whitesides, G. M. Soft Robotics for Chemists. *Angew. Chemie* **123,** 1930–1935 (2011).

46. Mosadegh, B. *et al.* Pneumatic Networks for Soft Robotics that Actuate Rapidly. *Adv. Funct. Mater.* **24,** 2163–2170 (2014).

47. Wang, B., Benitez, A. J., Lossada, F., Merindol, R. & Walther, A. Bioinspired Mechanical Gradients in Cellulose Nanofibril/Polymer Nanopapers. *Angew. Chemie - Int. Ed.* **55,** 5966–5970 (2016).

48. X. Gu, G. *et al.* Three-Dimensional-Printing of Bio-Inspired Composites. *J. Biomech. Eng.* **138,** 21006 (2016).

49. Rossetti, L. *et al.* The microstructure and micromechanics of the tendon–bone insertion. *Nat. Mater.* (2017). doi:10.1038/NMAT4863

50. Lee, T. Y., Roper, T. M., Jo, E. S., Guymon, C. A. & Hoyle, C. E. Influence of Hydrogen Bonding on Photopolymerization Rate of Hydroxyalkyl Acrylates. *Macromolecules* 3659–3665 (2004).

51. Odian, G. *Principles of Polymerization*. (John Wiley & Sons, Inc., 2004).

Chapter 4. Conclusion

Vat photopolymerization can be a versatile 3D printing technology, but lackluster options for multi-material printing, printing of elastomer materials, and printing of hydrophobic resins make vat photopolymerization unsuitable for many advanced rapid prototyping applications. We produced advancements in methodology and materials which attempt to address these shortcomings. We proposed new paradigms of multi-material vat photopolymerization which can exploit chemical principles, specifically polymerization kinetics and photoactivation wavelengths, to fabricate multi-material objects with full spatial control of material composition and options for compositional gradients. Using a biphasic mixture of immiscible liquids, we demonstrated that hydrophobic resins could be printed with excellent consistency with only a bed of water. We also introduced and printed accessible new elastomer photoresins which printed isotropically, showed modular and tunable property sets, and exhibited elongations to break over 300%. It is anticipated that this research will find application in fields such as soft robotics, wearable devices, and flexible electronics while enhancing the rapid prototyping capabilities of vat photopolymerization in general. Most importantly however, this research furthers a chemical understanding of vat polymerization processes and materials which can serve as a starting point for future innovations.